

Replica-symmetry breaking for directed polymers

Alexander K. Hartmann

Institut für Physik, Universität Oldenburg, 26111 Oldenburg, Germany

Directed polymers on 1+1 dimensional lattices coupled to a heat bath at temperature T are studied numerically for three ensembles of the site disorder. In particular correlations of the disorder as well as fractal patterning are considered. Configurations are directly sampled in perfect thermal equilibrium for very large system sizes with up to $N = L^2 = 32768 \times 32768 \approx 10^9$ sites. The phase-space structure is studied via the distribution of overlaps and hierarchical clustering of configurations. One ensemble shows a simple behavior like a ferromagnet. The other two ensembles exhibit indications for complex behavior reminiscent of multiple replica-symmetry breaking. Also results for the ultrametricity of the phase space and the phase transition behavior of $P(q)$ when varying the temperature T are studied. In total, the present model ensembles offer convenient numerical accesses to comprehensively studying complex behavior.

Disordered systems like structural glasses [1], spin glasses [2–7] or random optimization problems [8–10] exhibit for some ensembles of disorder realizations complex low-temperature phases, characterized by rough energy landscapes and diverging times scales. Most of such models cannot be solved analytically, except few mean-field ensembles like the Sherrington-Kirkpatrick (SK) spin-glass [11, 12]. By solving the SK model, a particular signature of complex behavior, *replica-symmetry breaking* (RSB), was introduced [13, 14]. Usually, and in the present work, the term RSB is used also for other systems exhibiting multi-level hierarchical and rough energy landscapes. On the numerical side [15] so far, the models, which show such complex behavior for ensembles with uncorrelated disorder, can be treated only with an exponentially growing running time, let it be Monte Carlo simulations [16] or ground-state calculations [17]. This prohibits a sophisticated analysis. On the other hand, for models where fast algorithms exist, e.g., random-field Ising systems [18], two-dimensional spin glasses [19], or matching problems [20], the behavior of uncorrelated or long-range power-law correlated disorder ensembles is simple [21–26], similar to a ferromagnet.

It is the purpose of the present paper to show that by using more sophisticated disorder ensembles, in particular with suitable correlations, indeed a complex behavior might be observed also for models where fast and exact algorithms exist, allowing one to treat very large system sizes. To be more precise, here the directed polymer in a random medium (DPRM) [27–29] on a two-dimensional disordered lattice was studied. This model allows for exact equilibrium sampling of configurations for huge lattices with even $N = 10^9$ sites. It is already known that directed polymers on random trees exhibit one-step RSB [30–32], but on finite-dimensional lattices with ensembles of uncorrelated disorder, no sign of complex behavior was found [33]. On the other hand, there are indications that by using another ensemble, originating from the Burger equation [34], a complex behavior may be found, and also more general approaches to complexity exist [35]. Motivated by these results, in this work, lines or segments

[36, 37] of distinct disorder values will be employed in a novel way to the DPRM problem. Here, a low temperature phase with a broad distribution of overlaps and a ultrametric organization of the phase space is present.

For the general two-dimensional case, each realization of the model [27, 28] is given by a lattice with $N = (L + 1) \times (L + 1)$ sites, open boundary conditions and local quenched energy potential values $\{V(x, y)\}$ for $x, y \in \{0, 1, \dots, L\}$. Directed polymers run from $(0, 0)$ to (L, L) and contain $2L + 1$ lattice sites $P = \{(x_\tau, y_\tau) | \tau = 0, \dots, 2L\}$ and are located on adjacent lattice sites always moving towards the final point (L, L) . Hence, for each “time” $\tau = x + y$, exactly one site is present in P , and for $(x, y) \in P$ with $x + y < 2L$ either $(x + 1, y) \in P$ or $(x, y + 1) \in P$. The energy of such a configuration is given by the sum $E(P) = \sum_{(x,y) \in P} V(x, y)$ of the potentials of the visited sites. The system is considered to be coupled to a heat bath at temperature T , such that each valid polymer exhibits a probability $e^{-E(P)/T}/Z$ with partition function $Z = \sum_P e^{-E(P)/T}$. The model allows for each disorder realization for a dynamic-programming, or transfer-matrix, calculation [27, 38, 39] of the partition function via site-dependent partition functions with $Z(0, 0) = e^{-V(0,0)/T}$ and for $x, y = 1, \dots, L$: $Z(x, 0) = Z(x - 1, 0)e^{-V(x,0)/T}$, $Z(0, y) = Z(0, y - 1)e^{-V(0,y)/T}$, and $Z(x, y) = (Z(x - 1, y) + Z(x, y - 1))e^{-V(x,y)/T}$. Note that $Z = Z(L, L)$. Z can be calculated in time $O(L^2)$. Furthermore, it is possible to sample polymer configurations in exact equilibrium by always starting with $P = P_0 \equiv \{(L, L)\}$. Then one adds further sites towards smaller times $\tau \rightarrow \tau - 1$ as follows: if the most recently added site is (x, y) , as next site either $(x - 1, y)$ is added to P , with probability $Z(x - 1, y)e^{-V(x,y)/T}/Z(x, y)$, else site $(x, y - 1)$, thus with probability $Z(x, y - 1)e^{-V(x,y)/T}/Z(x, y)$. If only one of the two sites is accessible, on the border of the lattice, this single site is included in P . This process finishes when the origin $(0, 0)$ is reached. Each sampling requires only $O(L)$ steps.

Here two ensembles are considered where most lattice sites have $V \equiv 0$ but in addition segments or lines [36, 37]

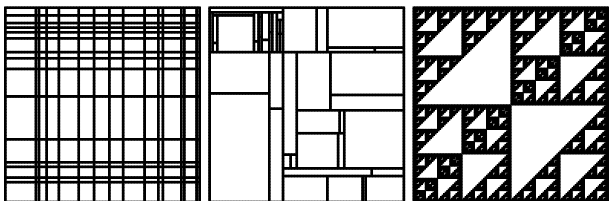


FIG. 1. Examples of disorder realizations ($L = 128$). White spaces correspond to potential $V = 0$, black blocks to $V = -1$. Shown are (left) *Hash* with 50 lines; (middle) *Mondrian* with 50 lines; (right) *Sierpinski* triangles.

on the lattice are introduced along which the potential has the same value $V = -1$, favoring pinning of the polymer at low temperatures [40]. Third, an “ensemble” containing a single fractal structure of potential values -1 and 0 is investigated.

Here lattice sizes with $L = L_k = 2^k$ are considered. Each lattice exhibits at the border a potential $V(x, y) \equiv -1$, i.e., for $x = 0$, $x = L$, $y = 0$ or $y = L$. There are more non-zero energy values, which are chosen for three ensembles, see Fig. 1. The ensembles *Hash* [36, 37], *Mondrian*, which is introduced in this work, and *Sierpinski*, are defined as follows

- *Hash*: A number s of randomly chosen straight segments of length L are added where $V \equiv -1$. This means, l times a random point $(x_0, 0)$ or $(0, y_0)$ is selected and $V(x_0, y) \equiv -1$ or $V(x, y_0) \equiv -1$ is assigned for all $x, y \in \{1, \dots, L-1\}$.
- *Mondrian*: A set D of straight segments is maintained, which contains initially the two segments $(0, 0) \rightarrow (0, L)$ and $(0, 0) \rightarrow (L, 0)$. Then s times a segment is drawn with uniform probability $1/|D|$ from the current set D , without removing it. A site (x_0, y_0) is selected uniformly on this segment. Then a new segment is added to D which starts at the site (x_0, y_0) and runs, perpendicular to the selected segment, until any other segment from D is hit. Finally, all sites belonging to the segments in D obtain $V \equiv -1$.
- *Sierpinski*: The discretized fractal Sierpinski structure with, for lattice size L_k , $k-2$ recursion levels is embedded on the lattice. All sites belonging to Sierpinski triangles obtain $V \equiv -1$.

For all ensembles, all other sites not having $V \equiv -1$, obtain $V \equiv 0$. Here, for lattice size $L = L_k$, $s_k = 10(k-5)$ segments are inserted, respectively. Thus, the minimum meaningful lattice size is $L_6 = 64$ for this study. Note that in Fig. 1 where $L = 128 = 2^7$ instead of $s_7 = 20$ a higher number of $s = 50$ segments is used, for better visibility.

Each polymer configuration P is characterized, first, by its energy $E(P)$ as defined above. This allows one to mea-

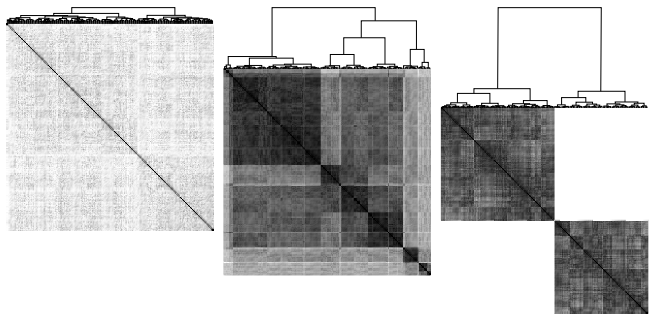


FIG. 2. Examples for clustered overlap matrices with dendrograms showing the structures of the configurations space, each time 200 sampled for one realization ($L = 16384, T = 0.5$). A black dot means $q = 1$ while white corresponds to $q = 0$. Shown are (left) *Hash* with 90 lines; (middle) *Mondrian* with 90 lines; (right) *Sierpinski* triangles.

sure in equilibrium the average energy $\langle E \rangle$ and the specific heat $C(T) = (\langle E^2 \rangle - \langle E \rangle^2) / (NT^2)$, for which one can also set up corresponding transfer-matrix equations [41]. For the random-disorder ensembles a linear average of all quantities over different realizations is performed, not indicated by separate brackets here. To characterize the model with respect to its energy landscape, the overlap q between two polymers P_1, P_2 is used [42], which is the fraction of joint sites, i.e., $q_{12} \equiv |P_1 \cap P_2| / (2L+1) \in [0, 1]$. By sampling many polymers in equilibrium, evaluating all (or many) overlaps, an approximation of the distribution $P(q)$ of overlaps is obtained.

To analyze the configuration space of these three ensembles, different disorder realization were studied first at temperature $T = 0.5$. System sizes ranging from $L = 64$ to $L = 32768$ were considered. A number of independent disorder realizations ranging from 2000 for the smallest size to 500 for the largest size were investigated. For each disorder configuration $M = 200$ independent polymer configurations were sampled in exact equilibrium.

The configuration space structure was analyzed by applying the an *agglomerative clustering approach* of Ward [43]. The hierarchical structure obtained by the clustering can be visualized by a tree, usually called *dendrogram*, where each branching corresponds to a subspace of configurations, see Fig. 2. The sequence of configurations as located in the leafs defines a partial order. This order can be used to display the matrix of the pair-wise overlaps where the order of the rows and columns is exactly given by the leaf order, see also Fig. 2. For the *Hash* ensemble, a rather gray uniform area is visible. This indicates that the configuration space is rather uniform, like a paramagnet. On the other hand, the matrices for the samples from *Mondrian* and *Sierpinski* display a block-diagonal structure, which is recursively visible inside the blocks as well. This is an indication for a complex configuration space, as it has been observed, e.g., for mean-field

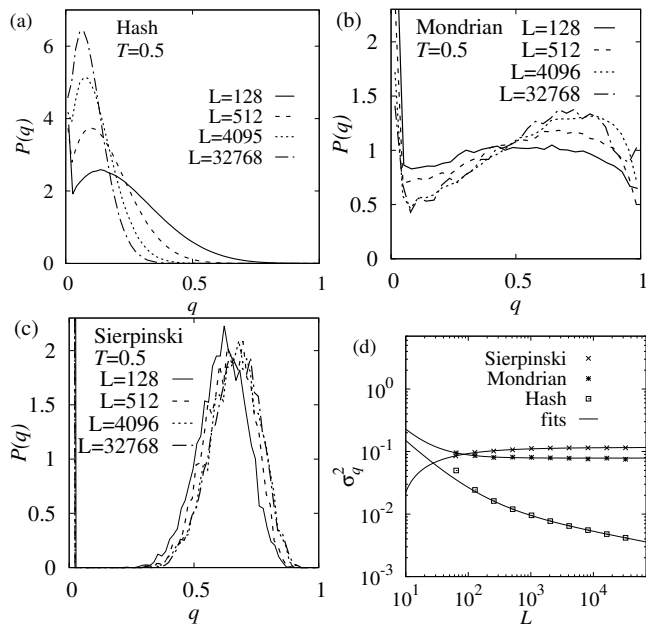


FIG. 3. Distribution $P(q)$ of overlaps at temperature $T = 0.5$ for four different system sizes. The results are for (a) *Hash*, (b) *Mondrian*, and (c) *Sierpinski* triangles. In (d) the variance σ_q^2 of these distributions for the three ensembles is shown as function of the system size N , together with fits (see text).

spin glass models [44] or solution-space landscapes of optimization problems [45, 46].

In Fig. 3 the distributions of overlaps are shown. For the *Hash* case, the distribution gets strongly narrower, indicating a convergence to $P(q) = \delta(q - q_0)$, which corresponds to a trivial configuration landscape. From a fit of the mean as function of L to a power-law plus constant q_0 , a value of $q_0 = 0.081(3)$ was obtained. On the other hand, for the other two ensembles $P(q)$ seems to converge to a broad distribution for $q > 0$ plus a delta-peak at $q = 0$ with some weight w_0 , which accounts for polymers having different paths right from the start. For the *Sierpinski* ensemble the data exhibits a convergence to $w_0 = 0.5$. This is compatible with the structure of the lattice, since at the starting site the paths either go down or right and never meet again, thus half of the pairs have zero overlap. For the *Mondrian* ensemble, a much smaller limiting zero-overlap peak-weight $w_0 \approx 0.04$ is found, i.e., most of the overlap distribution is located in the non-trivial part. Also shown in Fig. 3 are the variances σ_q^2 of the distributions of overlaps for the three ensembles. For the *Mondrian* and the *Sierpinski* ensembles, the variance seems to converge to finite values in the $L \rightarrow \infty$ limit. This is confirmed by good fits for $L > 100$ of the data to functions of the form $\sigma(N) = \sigma_\infty + aL^{-b}$ which lead to clear non-zero values $\sigma_\infty = 0.1163(8)$ for the *Sierpinski* ensemble and $\sigma_\infty = 0.0785(7)$ for the *Mondrian* ensemble. Thus, for these two ensembles the distribution of overlaps remains broad at low temperature in

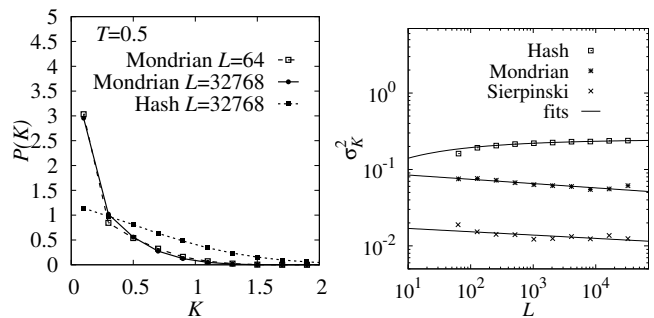


FIG. 4. (left) Sample distributions $P(K)$ of the ultrametricity measure for the *Mondrian*, and *Hash* ensembles. (Right) variance σ_K^2 of these distributions for the three ensembles as function of the system size N , together with fits (see text).

the thermodynamic limit $L \rightarrow \infty$ indicating a complex phase space structure. The variance for the *Hash* ensemble exhibits a positive curvature in the log-log plot, which could also be taken as indication for a complex structure. Nevertheless, here each polymer path can be decomposed in many sub paths with a high degree of independence, which speaks in favor of a simple configuration-space structure. Indeed, a limiting zero width is compatible: When fitting for $L > 100$ a power-law with a correction term, $\bar{\sigma}(N) = aL^{-b}(1 + eL^{-d})$, a good fit is obtained as well, as shown in the figure.

A hierarchical configuration space, like for the SK model, is characterized by an *ultrametric* structure [47], i.e., an underlying tree. To characterize ultrametricity, one considers triples of configurations P_1, P_2 , and P_3 and their mutual overlaps q_{12}, q_{13} , and q_{23} which are, without loss of generality, ordered such that $q_{12} \leq q_{13} \leq q_{23}$. For a true ultrametric space, for an infinite system size, $q_{12} = q_{13}$ would hold. To characterize the emergence of ultrametricity here, the quantity $K = (q_{13} - q_{12})/\sigma_q$ is used [44], where σ_q is the width of the overlap distribution $P(q)$. For a non-trivial ultrametric organization, the distribution $P(K)$ should converge to a delta-function $\delta(K)$, i.e., a variance σ_K^2 which converges to zero. In the left of Fig. 4 samples for $P(K)$ are shown for *Mondrian* and *Hash* ensembles. The former one exhibits a slight change towards smaller values of K when increasing the system size L . For the latter one, the distribution is much broader, also for the largest considered size. This is confirmed by the behavior of the variance σ_K^2 of these distributions as function of the system size. The data is compatible with a gentle power-law decreases, shown as straight lines, for the *Mondrian* and the *Sierpinski* ensembles. This can be expected for the fractal *Sierpinski* ensemble since it has an obvious hierarchical structure. Note that the convergence even in this obvious ultrametric case is slow, as it was also observed for long-range spin glasses exhibiting RSB [44]. Thus, the data indicates that also the *Mondrian* ensemble exhibits ultrametricity as well. Also, the variance seems to con-

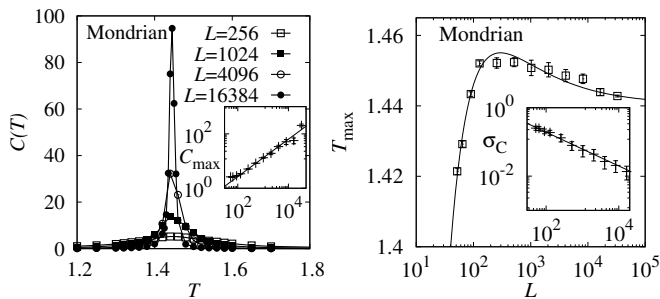


FIG. 5. (left) Specific heat $C(T)$ as function of temperature for the *Mondrian* ensemble and four different system sizes. The inset shows the peak height C_{\max} as function of the system size. (right) Position T_{\max} of the peak of $C(T)$ as function of system size L and in the inset the width σ_C of the peak. The lines for $C(T)$ are guide to the eyes, the other lines display fits (see text).

verge to a constant for the *Hash* ensemble, compatible with the absence ultrametricity, and expected because of the simpler distribution of overlaps.

In order to study the temperature dependence [41] of an ensemble with complex behavior, for *Mondrian*, a large number of simulations was performed. Note that similar simulations for the Sierpinski model exhibited hard to analyze discontinuities and are thus not presented here. Lattice sizes $L \leq 16384$ for many temperatures $T \in [0.1, 3]$, plus for $L = 32768$ for few temperatures near the estimated critical point were considered with the number of disorder samples between 500 and 1000. In the left of Fig. 5 examples for the specific heat $C(T)$ behavior is shown. Clearly peaks are visible near $T \approx 1.4$, growing and narrowing with increasing system size, indicating a phase transition. For a second order phase transition [48–51] one would expect that the specific heat scales as

$$C(T, L) = L^{\alpha/\nu} \tilde{c}((T - T_c)L^{1/\nu}), \quad (1)$$

with a size-independent function $\tilde{c}()$ and critical exponents ν , describing the divergence of the correlation length, and α describing the divergence of the specific heat. Indeed, the height of the peak follows clearly a power law $C_{\max}(L) \sim L^{\alpha/\nu}$, see inset of the left Fig. 5. A fit to this power law results in $\alpha/\nu = 0.69(2)$.

The position T_{\max} of the peak was estimated by fitting Gaussians near the peak. The position as a function of the system size is shown in the right of Fig. 5. Only a weak, third-digit significant, but non-monotonous size dependence is visible. Equation (1) means that scaling of the peak position leads to a leading behavior $T_{\max}(N) - T_c \sim L^{-1/\nu}$. Nevertheless, fitting just a power law does not work well, even when restricting to larger sizes. On the other hand, Eq. (1) also concerns the shape of the specific heat, i.e., the width of the peak region should also scale like $L^{-1/\nu}$. The width, as obtained also from the Gaussian fits, shows indeed a clear power law. A fit to a power law, yielded $\nu = -2.02(8)$.

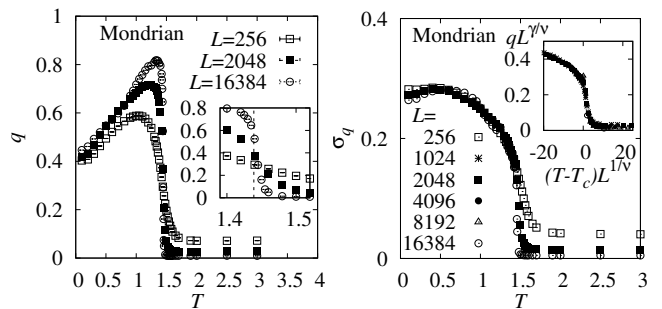


FIG. 6. *Mondrian* ensemble and different system sizes in the (left) the mean overlap $q(T)$ as function of temperature. The inset shows the data near the estimated transition point, indicated by a vertical dashed line. (right) mean width $\sigma_q(T)$ of the overlap distribution, for three sample system sizes The inset shows the rescaled data for system sizes $L \geq 1024$.

When fixing ν to this value, a fit to a power-law with correction $T_{\max}(N) = T_c + cL^{-1/\nu}(1 + dL^{-\omega})$ yields a reasonable fit, see Fig. 5, with $T_c = 1.439(8)$. With this value of ν , a rather large value of $\alpha \approx 1.4$ results, which could indicate that actually a first-order phase transition is behind the seen data [52]. This is compatible with the observed discontinuities of the related Sierpinski lattice.

The average overlap $q(T)$ is shown in the left of Fig. 6. At low temperatures $T > T_c$, the average overlap is non-zero. The curves for different system sizes cross near T_c and just below T_c the average overlap grows with the system size. This is an unusual behavior when comparing, e.g., with a ferromagnet. A data collapse (not shown) leads to an unphysical negative critical exponent. Note that also the average squared overlap (not shown) exhibits this behavior. The average width $\sigma_q(T)$ of the overlap distribution is shown in the right of Fig. 6. The data can be rescaled reasonably well, see inset, according to $\sigma_q(T, L) = L^{-\gamma/\nu} \tilde{\sigma}((T - T_c)L^{1/\nu})$ when using the values $T_c = 1.439$, $\nu = 2.02$ obtained already and estimating $\gamma/\nu = 0.07(2)$. The smallest system sizes are excluded from the collapse due to too large finite-size corrections. $L = 32768$ is not included here due to bad statistics.

To conclude, it was shown that some specific ensembles of the disorder for random polymers on a two-dimensional lattice, at low temperatures exhibit a complex hierarchical organization of the phase space, similar to RSB. In contrast to other models exhibiting complex behavior, the present models allows for fast and exact sampling at arbitrary temperatures, i.e., to study large system in true equilibrium. This may open a path, by just using suitably correlated disorder ensembles, to study in a numerically convenient way complex behavior. This may be done for other disorder ensembles, other lattice dimensions or even other models where exact equilibrium sampling is possible.

The author thanks A. Peter Young, Hendrik Schawe and Phil Krabbe for critically reading the manuscript

and useful discussions. The simulations were performed at the the HPC cluster CARL, located at the University of Oldenburg (Germany) and funded by the DFG through its Major Research Instrumentation Program (INST 184/157-1 FUGG) and the Ministry of Science and Culture (MWK) of the Lower Saxony State.

-
- [1] L. Berthier and G. Biroli, *Rev. Mod. Phys.* **83**, 587 (2011).
- [2] K. Binder and A. Young, *Rev. Mod. Phys.* **58**, 801 (1986).
- [3] M. Mézard, G. Parisi, and M. Virasoro, *Spin glass theory and beyond* (World Scientific, Singapore, 1987).
- [4] K. H. Fischer and J. A. Hertz, *Spin Glasses* (Cambridge University Press, Cambridge, 1991).
- [5] A. P. Young, ed., *Spin glasses and random fields* (World Scientific, Singapore, 1998).
- [6] H. Nishimori, *Statistical Physics of Spin Glasses and Information Processing: An Introduction* (Oxford University Press, Oxford, 2001).
- [7] N. Kawashima and H. Rieger, in *Frustrated Spin Systems*, edited by H. T. Diep (World Scientific, 2013) 2nd ed., pp. 509–614.
- [8] A. K. Hartmann and M. Weigt, *Phase Transitions in Combinatorial Optimization Problems* (Wiley-VCH, Weinheim, 2005).
- [9] M. Mézard and A. Montanari, *Information, Physics and Computation* (Oxford University Press, Oxford, 2009).
- [10] C. Moore and S. Mertens, *The Nature of Computation* (Oxford University Press, Oxford, 2011).
- [11] D. Sherrington and S. Kirkpatrick, *Phys. Rev. Lett.* **35**, 1792 (1975).
- [12] M. Talagrand, *Ann. Math.* **163**, 221 (2006).
- [13] G. Parisi, *Phys. Rev. Lett.* **43**, 1754 (1979).
- [14] G. Parisi, *Phys. Rev. Lett.* **50**, 1946 (1983).
- [15] A. K. Hartmann, *Big Practical Guide to Computer Simulations* (World Scientific, Singapore, 2015).
- [16] M. E. J. Newman and G. T. Barkema, *Monte Carlo Methods in Statistical Physics* (Clarendon Press, Oxford, 1999).
- [17] A. K. Hartmann and H. Rieger, *Optimization Algorithms in Physics* (Wiley-VCH, Weinheim, 2001).
- [18] A. T. Ogielski, *Phys. Rev. Lett.* **57**, 1251 (1986).
- [19] F. Barahona, R. Maynard, R. Rammal, and J. Uhry, *J. Phys. A* **15**, 673 (1982).
- [20] T. H. Cormen, S. Clifford, C. E. Leiserson, and R. L. Rivest, *Introduction to Algorithms* (MIT Press, Cambridge (USA), 2001).
- [21] M. Mézard and G. Parisi, *Journal de Physique* **48**, 1451 (1987).
- [22] A. A. Middleton and D. S. Fisher, *Phys. Rev. B* **65**, 134411 (2002).
- [23] A. K. Hartmann and M. A. Moore, *Phys. Rev. Lett.* **90**, 127201 (2003).
- [24] A. K. Hartmann and M. A. Moore, *Phys. Rev. B* **69**, 104409 (2004).
- [25] B. Ahrens and A. K. Hartmann, *Phys. Rev. B* **84**, 144202 (2011).
- [26] L. Münster, C. Norrenbrock, A. K. Hartmann, and A. P. Young, *Phys. Rev. E* **103**, 042117 (2021).
- [27] M. Kardar and Y.-C. Zhang, *Phys. Rev. Lett.* **58**, 2087 (1987).
- [28] D. S. Fisher and D. A. Huse, *Phys. Rev. B* **43**, 10728 (1991).
- [29] T. Halpin-Healy and Y.-C. Zhang, *Phys. Rep.* **254**, 215 (1995).
- [30] B. Derrida and H. Spohn, *J. Stat. Phys.* **51**, 817– (1988).
- [31] M. Mézard and G. Parisi, *J. de Physique I* **1**, 809 (1991).
- [32] B. Derrida and P. Mottishaw, *Europhys. Lett.* **115**, 40005 (2016).
- [33] M. Ueda, *Journal of Statistical Mechanics: Theory and Experiment* **2019**, 053302 (2019).
- [34] M. Ueda and S.-i. Sasa, *Phys. Rev. Lett.* **115**, 080605 (2015).
- [35] S. Franchini, “Replica symmetry breaking without replicas,” (2019), arXiv:1610.03941 [cond-mat.stat-mech].
- [36] A. Weinrib and B. I. Halperin, *Phys. Rev. B* **27**, 413 (1983).
- [37] H. Meier, M. Wallin, and S. Teitel, *Phys. Rev. B* **87**, 214520 (2013).
- [38] D. A. Huse and C. L. Henley, *Phys. Rev. Lett.* **54**, 2708 (1985).
- [39] M. Kardar, *Phys. Rev. Lett.* **55**, 2235 (1985).
- [40] G. Giacomin and F. L. Toninelli, *Commun. Math. Phys.* **266**, 1 (2006).
- [41] B. Derrida and O. Golinelli, *Phys. Rev. A* **41**, 4160 (1990).
- [42] S. Mukherji, *Phys. Rev. E* **50**, R2407 (1994).
- [43] The clustering approach [53, 54] operates on a set of M sampled configurations by initializing a set of M clusters each containing one configuration. One maintains pairwise distances between all clusters, which are initially the distances between the configurations. Then iteratively two clusters exhibiting the currently shortest distance between them are selected and merged to one single cluster, thereby reducing the cluster number by one. For this new merged cluster, an updated distance to all other still existing clusters have to be obtained. Here the update is done with the approach of Ward [53], which has been used previously for the analysis of disordered systems [44–46], for more details see there. The merging process is iterated until only one cluster is left.
- [44] H. G. Katzgraber and A. K. Hartmann, *Phys. Rev. Lett.* **102**, 037207 (2009).
- [45] W. Barthel and A. K. Hartmann, *Phys. Rev. E* **70**, 066120 (2004).
- [46] A. Mann and A. K. Hartmann, *Phys. Rev. E* **82**, 056702 (2010).
- [47] R. Rammal, G. Toulouse, and M. A. Virasoro, *Rev. Mod. Phys.* **58**, 765 (1986).
- [48] H. E. Stanley, *An Introduction to Phase Transitions and Critical Phenomena* (Oxford University Press, Oxford, 1971).
- [49] N. Goldenfeld, *Lectures on phase transitions and the renormalization group* (Addison-Wesely, Reading (MA), 1992).
- [50] J. Cardy, *Scaling and Renormalization in Statistical Physics* (Cambridge University Press, Cambridge, 1996).
- [51] J. M. Yeomans, *Statistical mechanics of phase transitions* (Clarendon Press, Oxford, 2002).
- [52] In renormalization group studies one obtains for a d -dimensional system $\alpha = 2 - d/y_1$. For a first-order phase transition $y_1 = d$ holds [55], which leads to $\alpha = 1$ which is large compared to typically observed values.
- [53] J. Ward, *J. of the Am. Stat. Association* **58**, 236 (1963).

[54] A. K. Jain and R. C. Dubes, *Algorithms for Clustering Data* (Prentice-Hall, Englewood Cliffs, USA, 1988).

[55] B. Nienhuis and M. Nauenberg, Phys. Rev. Lett. **35**, 477 (1975).